Energetic electrons emitted from ethanol droplets irradiated by femtosecond laser pulses

X. Y. Peng, J. Zhang,* and Z. Jin

Laboratory of Optical Physics, Institute of Physics, Chinese Academy of Sciences, Beijing 100080, China

T. J. Liang

Research Institute of Chemical Defenses, Beijing 102205, China

Z. M. Sheng, Y. T. Li, Q. Z. Yu, Z. Y. Zheng, Z. H. Wang, and Z. L. Chen

Laboratory of Optical Physics, Institute of Physics, Chinese Academy of Sciences, Beijing 100080, China

J. Y. Zhong

Laboratory of Optical Physics, Institute of Physics, Chinese Academy of Sciences, Beijing 100080, China
and National Astronomical Observatories, Chinese Academy of Sciences, Beijing 100012, China

X. W. Tang

Department of Physics, Zhejiang University, Hangzhou 310027, China

J. Yang and C. J. Sun

Department of Technical Physics, Peking University, Beijing 100080, China

We investigate the angular distribution and the energy spectrum of hot electrons emitted from ethanol droplets irradiated by linearly polarized 150-fs laser pulses at an intensity of 10^{16} W/cm^2. Two hot electron jets symmetrically with respect to the laser propagation direction are observed within the polarization plane. This is due to the spherical geometry of droplets in the intense laser field. The maximum energy of the hot electrons is found to be more than 600 keV. Particle-in-cell simulations suggest that the resonance absorption is the main mechanism for hot electron generation.

I. INTRODUCTION

Along with the development of ultrashort high-power laser technologies [1,2], laser-matter interactions have been investigated extensively. Using ultrashort high-power lasers, energetic particles and radiations such as fast electrons [3–5], high-energy ions [6–8], neutrons [9,10], and x rays [11,12] have been generated in laser-solid and laser-cluster interactions over the past years. Recently, the interaction between ultrashort high-power laser pulses and droplets has attracted significant attention. Because these droplets are at a near-solid density but with micron-scale sizes that are comparable to the wavelength of visible light, high laser absorptions and strong laser-plasma interactions are found, where the absorbed energy does not lose to its surroundings through rapid conduction processes [13]. Therefore, the resulting hot droplets show the prospect of being new sources of x rays, protons, and even neutrons [13–17]. The absorption of laser energy and the emission of hard x rays, white light, soft x rays, and extreme ultraviolet (EUV) light in the laser-droplet interactions have been studied [13,15,16]. However, only a few publications are involved in the study of hot electron generation from the droplets, and in particular, there is no direct measurement of the energy spectrum of energetic elec-

trons and their angular distributions. These measurements can help to clarify the mechanism of the hot electron generation.

In this paper we report measurements of the angular distribution and energy spectrum of hot electrons from ethanol droplets irradiated by linearly polarized 150-fs laser pulses at intensity around 10^{16} W/cm^2. The results suggest that resonance absorption is the primary mechanism producing hot electrons.

II. EXPERIMENTAL SETUP

The experiments were carried out at the Laboratory of Optical Physics in the Institute of Physics with a Ti: sapphire chirped pulse amplification (CPA) laser system operating at a wavelength around 790 nm at a repetition rate of 10 Hz. Figure 1 shows the schematic of the experimental setup. The laser delivered 5 mJ energy in 150-fs pulses with a peak-to-pedestal contrast ratio of 10^5 at 20 ps before the peak measured by a third-order autocorrelator. A linearly polarized laser beam (with a polarization ratio of 95%) was focused with an 80-mm-focal-length lens, yielding a peak intensity around 10^{16} W/cm^2 at the focus with a diameter of about 20 μm. The electric field vector of the laser pulses was parallel or perpendicular to the horizontal plane by rotating a half-wave plate.

A pulsed valve was used to generate ethanol droplets. This system consists of a gas line backed with high-pressure

---

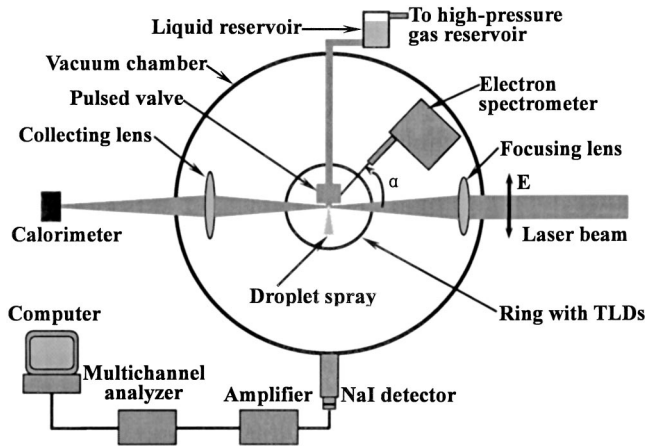*Author to whom correspondence should be addressed; electronic address: jzhang@aphy.iphy.ac.cn

FIG. 1. (Color online) Schematic of experimental setup used for the laser-droplet interaction.
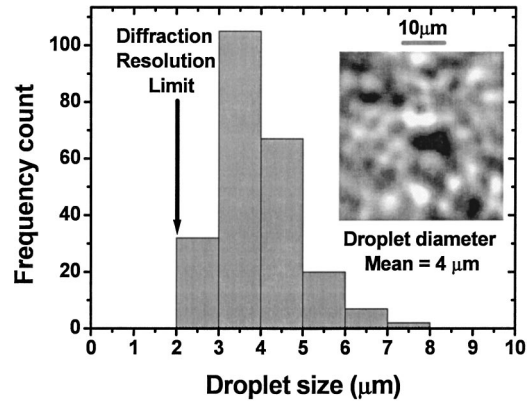

FIG. 2. (Color online) Histogram of the droplet diameter distribution from ethanol droplet spray ($T=300$ K, backing pressure 20 atm) imaged using 395-nm laser pulses. The inset shows a typical image of the droplet stream. The mean diameter is about 4 μm.

nitrogen (at 20 atm), a liquid reservoir with ethanol in it, and a solenoid-driven pulsed valve with a 100-μm orifice. The valve was pulsed for 460 μs at a repetition rate of 10 Hz. The high-pressure gas along the line propelled the ethanol over the liquid reservoir to stream through the orifice. Thus high-density, polydisperse sprays containing several-micron-size ethanol droplets were formed in vacuum. The temperature of the valve was about 300 K.

The main diagnostic used for a direct measurement of the hot electron spectrum was a magnetic spectrometer. An array of LiF thermoluminescent dosimeter (TLD) pieces (type GR-200F) was used as detectors. The energy range of this instrument was from 20 keV to 2 MeV.

The angular distribution of hot electron emission was measured with an array of TLD's (type GR-200A) attached inside a ring. The TLD detectors were wrapped with a 20-μm-thick aluminum foil. This Al foil can block energetic ions, scattered laser light, soft x rays, and electrons with energies below 50 keV. Hard x rays can penetrate through the Al foil and TLD's. Thus, fast electrons with energies over 50 keV mainly contributed to the dosage recorded by the TLD's. The ring detector was placed in the polarization plane of the laser beam under the orifice and its center was in the same position as the laser focus. The angular resolution of this system is about 7°.

In order to get a true image of angular distributions of hot electrons from droplets, the main laser beam was focused in the center of the droplet spray at 3 mm under the orifice. The focusing condition in the center of the spray was monitored using a γ-ray spectrometer and a calorimeter. The γ-ray spectrometer consists of a NaI detector, an electronic gated shutter, a photomultiplier, an amplifier, and a multichannel energy analyzer. Using this system, x-ray bremsstrahlung radiation from the laser plasma can be monitored simultaneously. The calorimeter was used to measure the attenuation of the laser beam through the droplet spray. An $f/3$ lens was used to collect the penetrated lights through the spray and forward-scattered lights before the calorimeter.

The droplet size was measured using an optical imaging system. The droplet spray from the 100-μm-diam orifice was backilluminated with the frequency-doubled laser beam and

the shadows were magnified and imaged to a charge coupled device (CCD) camera. The spatial resolution of the imaging system was approximately 2.0 μm. A histogram of the size distribution of droplets, shown in Fig. 2, was compiled over many shots. The inset shows a typical magnified image of the droplet spray. The mean droplet diameter is about 4 μm. The number density of the spray, N, can be determined by measuring the rate at which liquid flows through the orifice and is dispersed into a given volume [18]. Therefore the atomic number density N_a of the spray can be determined as follows: $N_a=(n_a N \; \rho 4/3\pi r^3)/(mu)$, where ρ, m, u, n_a, and r represent the liquid ethanol density, molecular mass, atomic mass unit, number of atoms per molecule, and droplet radius, respectively. In our experiments, the number density and atomic number density of the spray at 3 mm under the orifice were $\sim 2.1\times10^8$ droplets/cm^3 and $\sim 1.8\times10^{21}$ atoms/cm^3, respectively.

III. RESULTS AND DISCUSSION

The angular (α) distribution, relative to the laser axis, of hot electrons with energies over 50 keV is shown in Fig. 3. The dose was accumulated over 18 000 shots. First, the main laser beam was focused in the center of the droplet spray at about 3 mm below the orifice with the laser polarization parallel to the horizontal plane. Two jets of hot electrons were found symmetric with respect to the laser axis as shown in Fig. 3(a). The angles of the two strongest emission directions of hot electrons with respect to the laser axis are about $-71°$ and $72°$, respectively. Fitting the data to Gaussian distributions, the full widths at half maximum (FWHM) of the two peaks are found to be about 60° for both of them. When the laser polarization direction was varied to be perpendicular to the horizontal plane by rotating the half-wave plate, hot electron emission behaved differently as shown in Fig. 3(b). This suggests that hot electrons only emit in the laser polarization plane and the angular distribution of hot electrons strongly depends on the laser polarization. From Fig. 3 one can also find that there were not only backward emissions ($-90°\leq\alpha\leq90°$) but also forward emissions
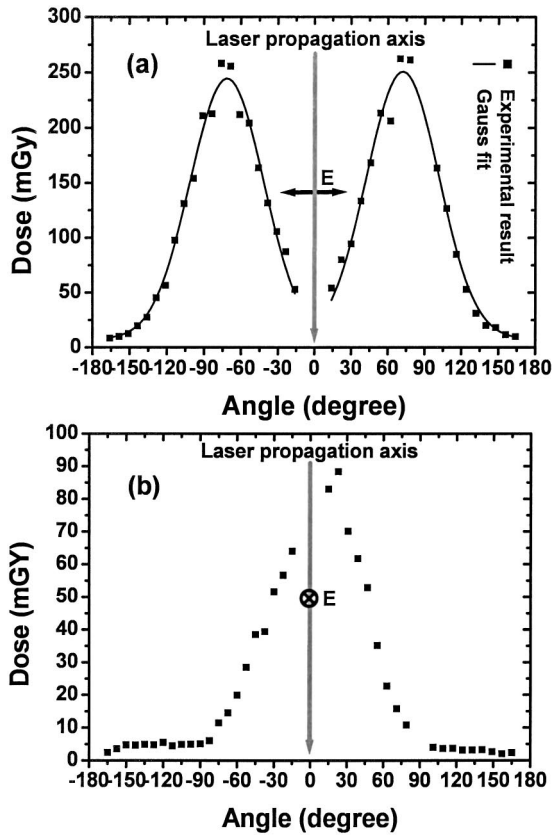
FIG. 3. The angular distributions of hot electrons with energies over 50 keV from ethanol droplets irradiated by a linearly polarized laser in the horizontal plane. The polarization plane of the laser beam is parallel to the horizontal plane in (a) and perpendicular to the horizontal plane in (b). The laser intensity and pulse duration are 10^{16} W/cm^2 and 150 fs, respectively. The two strongest emissions of hot electrons symmetrical with respect to the laser axis in (a) are about $-71°$ and $72°$, respectively.

$(90° \leqslant \alpha \leqslant 270°)$ of hot electrons. However, the latter are much weaker than the former. This means that the laser-droplet interaction generates not only outgoing hot electrons from the droplet surface but also injecting ones. The latter are absorbed and attenuated by the droplets themselves.

An electron spectrometer was placed in the position where its entrance hole was aligned to an angle of about 50° (see the angle of α in Fig. 1). Figure 4 shows the obtained energy spectrum of hot electrons from ethanol droplets under the same conditions as those in Fig. 3(a). The background radiation was deducted from all data. The mean background radiation of TLD's is 7 μGy (1 Gy is the radiation dose of one joule of energy absorbed per kilogram of matter). The following features are found from Fig. 4: (1) the maximum energy of hot electrons is over 600 keV, (2) the number of hot electrons with energies over 300 keV is very low as compared with those with energies less than 300 keV, and (3) the peak of the electron spectrum is around 120 keV. This implies that a charge separation potential was developed and many hot electrons had been pushed back to the droplet surface. Fitting the data to the Maxwellian distribution, an effective temperature of hot electrons, 56 keV, is obtained.
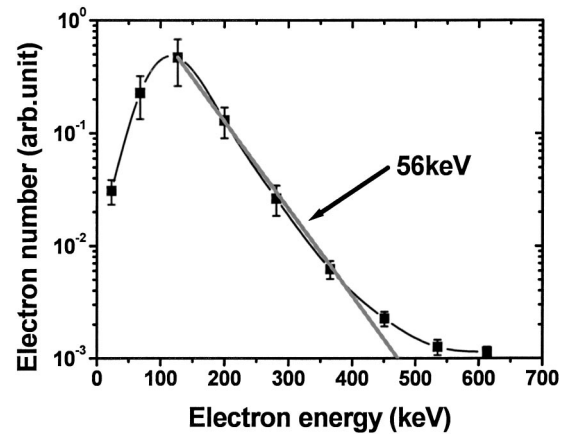

FIG. 4. Energy spectrum of hot electrons emitted from ethanol droplets, measured using a magnetic electron spectrometer. An effective temperature is obtained by fitting it with a Maxwellian distribution. The experimental conditions are the same as those in Fig. 3(a).

This temperature is comparable to the one (66 keV) obtained in laser-solid interactions under similar conditions [3]. It is also comparable to the one (70 keV) found in laser-cluster interactions under the condition that the atomic cluster be irradiated by a laser pulse at a higher intensity (10^{17} W/cm^2) but with a shorter duration (28 fs) [5].

The acceleration mechanisms of hot electrons in the laser-plasma interaction are different for different experimental conditions. Under our experimental conditions (150 fs, 10^{16} W/cm^2), classical collisional absorption is not the main mechanism for hot electron production, which might be responsible for the generation of plentiful thermal electrons with energies less than keV at modest laser intensities [19]. Collisionless absorption includes resonance absorption [20], vacuum heating (or the Brunel absorption) [21], abnormal skin effects [22], and pondermotive $\mathbf{J} \times \mathbf{B}$ heating [23]. In our experiments, since the intensity of laser pulse is much less than the relativistic laser intensity ($\sim 10^{18}$ W/cm^2), abnormal skin effects and the $\mathbf{J} \times \mathbf{B}$ heating cannot make a large contribution to the energetic electrons. Furthermore, parametric instabilities cannot be developed sufficiently under our experimental conditions because the experiments have not shown clear evidence of 3 $\omega_0/2$ harmonic emission.

We suggest that resonance absorption and vacuum heating might be mainly responsible for the hot electron production due to its strong dependence on the laser polarization in our case. Because a droplet has a unique sphere geometry, no matter with what kind of polarization the laser beam is, it has an electric field component along the direction of a density gradient pointing radially when it irradiates on the droplet. Therefore it is possible for the resonance absorption to occur on the critical surface, where an electron plasma wave can be stimulated and electrons can be accelerated in the direction of the density gradient. When the wave breaks, hot electrons can be produced [24]. On the other hand, because of the spatial dimension of the droplet at the micron scale, its characteristic explosion time (ps scale) is longer than the duration of the main laser pulse (150 fs); the laser plasma can sustain

a high density during the laser interaction. The electrons on the surface of the plasma droplet can be pulled quickly out into vacuum by the laser electric field and then are pushed back to the plasma with approximately the quiver velocity ($v_{osc} = eE/m_e\omega$) when the electric field reverses its sign. These electrons will then deposit their quiver energy into the overdense plasma where the laser electric field cannot penetrate. Thus it is possible to produce hot electrons from droplets via vacuum heating as well.

Gibbon and Bell investigated the interaction between sub-picosecond, obliquely incident laser light ($I\lambda^2 = 10^{14} - 10^{18}$ W/cm^2 μm^2) with solid targets [25]. He found that vacuum heating dominates over resonance absorption for scale lengths $L/\lambda < 0.1$, while resonance absorption plays a major role when $L/\lambda > 0.1$. This theory can be used to analyze our experimental results because the droplet has a similar density as a solid. Though the duration of the main pulse is 150 fs in our experiments, the prepulse starts about 20 ps at an intensity of 1×10^{11} W/cm^2 before the main pulse. The plasma density scale length L during this time can be calculated by using the one-dimensional (1D) Lagrangian hydrodynamic code MED103 [26]. For the sake of simplicity, a 4-μm-thick flat target instead of a spherical one was used. In the calculation of the ionization of the plasma we set $Z = 2.9$ and $A = 5.1$ for ethanol in the nonequilibrium average atom model. The result reveals that the size of the preplasma is about 0.7 μm. So we have $L/\lambda \sim 0.9 > 0.1$. According to the Gibbon-Bell theory, the resonance absorption dominates over the vacuum heating in our experiments.

To explain our experimental results, 2D particle-in-cell (PIC) simulations are performed, where the spherical droplets are approximated as infinitely long cylinders. The simulation box size is $25\lambda \times 30\lambda$. In the simulations we take $a_0 = 0.1$, which corresponds to a laser intensity at focus slightly larger than 10^{16} W/cm^2 used in our experiment. The laser pulse is incident along the x direction from left normally on to the droplet plasma with a diameter of 5 λ. Initially the electron density increases exponentially along the radial direction of the droplet from $0.2n_c$ at the droplet edge ($r = 2.5\lambda$ from the droplet center) until $2.0n_c$ at $r = 0.5\lambda$ where n_c is the critical density. The electron density remains at $2.0n_c$ from $r = 0.5\lambda$ until to the droplet center. The corresponding density scale length below the critical density is $L = 0.9\lambda$. Figure 5 illustrates the simulation results at the 50 laser cycles for a droplet plasma irradiated by a linearly polarized laser pulse with its polarization along the y direction. We find that both the longitudinal and transverse components of the excited electric field near the critical surface increase with time. When $t = 50$ laser cycles, these electric fields reach the maximum, which are much stronger than the incident laser electric field. Figures 5(a) and 5(b) display the longitudinal and transverse components of the resonantly excited electric field at the 50 laser cycles, respectively. It is exactly the enhanced oscillating electric field around the critical density surface that accelerates the electrons to high energies. Such electrons can overcome the electrostatic field induced in front of the droplet and be detected by the magnetic spectrometer. Figures 5(c) and 5(d) show the electron density profile and the spatial distribution (x-y plot) of the
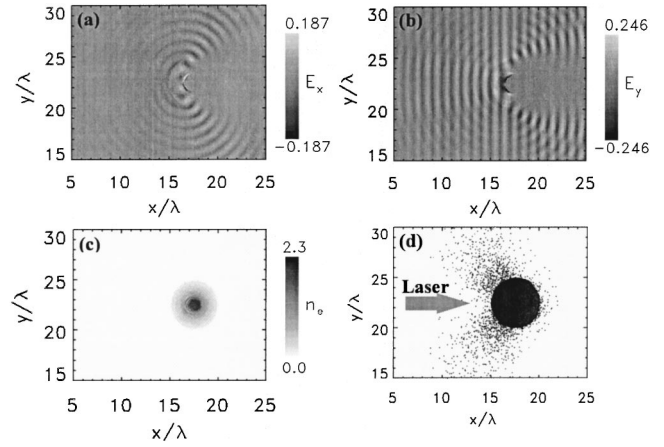

FIG. 5. Snapshots of 2D PIC simulation resulting at the 50 laser cycles for a plasma droplet irradiated by a linearly polarized laser pulse with its polarization along the y direction. (a) The longitudinal component of the resonantly excited electric field, (b) the transverse component of the electric field, (c) electron density profile, and (d) plot (x,y) of the electron positions.

electrons, respectively. We find that electron jets can be seen outgoing from the droplet surface after about 40 laser cycles. At 50 laser cycles, it is very apparent that two group electrons are accelerated to high energies symmetrically with respect to the laser axis from Fig. 5(d). The strong emissions range from $\pm 40°$ to about $\pm 90°$. This agrees well with the angular distribution measured in our experiments.

Figure 6 shows the energy spectrum of electrons with the density scale length $L = 0.9\lambda$ after 80 laser cycles obtained from the PIC simulations. This typical electron energy distribution can be approximated with a bitemperature Maxwellian distribution. The lower-energy electrons simply represent the initial thermal distribution and the higher-energy Maxwellian component represents the resonantly heated electrons. The temperature of the resonantly heated electrons is 65 keV, which is similar to our experimental result (56 keV). Our simulation results agree well with our measurements and confirm that resonance absorption is
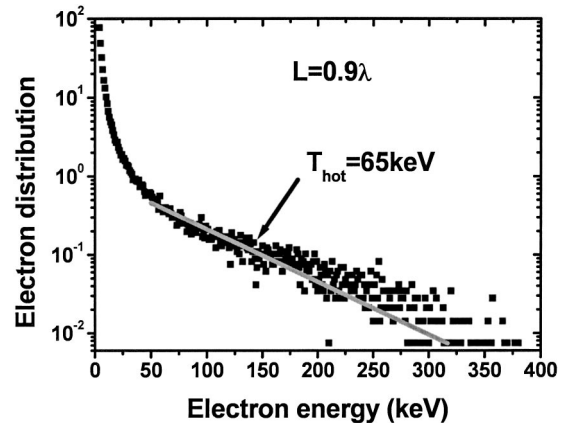

FIG. 6. The electron energy spectrum of a plasma droplet with density scale length $L = 0.9\lambda$ after interaction with the laser pulse for 80 laser cycles obtained from the PIC simulations.

mainly responsible for the angular distributions of hot electrons in our experiments.

IV. CONCLUSION

In conclusion, we have directly measured the angular distribution and energy spectrum of hot electrons from ethanol droplets irradiated by linearly polarized laser pulses with a duration of 150 fs at the intensity of 10^{16} W/cm^2. We observe a symmetric structure of the angular distribution of hot electrons with energies over 50 keV and two symmetric peaks of emission directions in large angles from ethanol droplets with respect to the laser axis. The temperature of hot electrons emitted from several-micron-size droplets is found to be comparative to that from solid and cluster targets under similar laser parameters. Both the measurements and the 2D PIC simulations suggest that resonance absorption mainly contributes to hot electron generation in laser-droplet interactions.

[1] D. Strickland and G. Mourou, Opt. Commun. **56**, 219 (1985).
[2] M. D. Perry and G. Mourou, Science **264**, 917 (1994).
[3] Y. T. Li *et al.*, Phys. Rev. E **64**, 046407 (2001).
[4] W. P. Leemans *et al.*, Phys. Rev. Lett. **89**, 174802 (2002).
[5] L. M. Chen *et al.*, Phys. Plasmas **9**, 3595 (2002).
[6] K. Krushelnick *et al.*, Phys. Rev. Lett. **83**, 737 (1999).
[7] A. Maksimchuk *et al.*, Phys. Rev. Lett. **84**, 4108 (2000).
[8] V. Kumarappan *et al.*, Phys. Rev. Lett. **87**, 085005 (2001).
[9] B. M. Smirnov, J. Phys. D **33**, 115 (2000).
[10] T. Ditmire *et al.*, Nature (London) **386**, 54 (1997).
[11] A. Mcpherson *et al.*, Nature (London) **370**, 631 (1994).
[12] H. Schwoerer, Phys. Rev. Lett. **86**, 2317 (2001).
[13] E. T. Gumbrell *et al.*, Phys. Plasmas **8**, 1329 (2001).
[14] S. J. Mcnaught *et al.*, Appl. Phys. Lett. **79**, 4100 (2001).
[15] Catherine Favre *et al.*, Phys. Rev. Lett. **89**, 035002 (2002).
[16] Kurt Garloff *et al.*, Phys. Rev. E **66**, 036403 (2002).
[17] S. Karsch *et al.*, Phys. Rev. Lett. **91**, 015001 (2003).
[18] L. C. Mountford *et al.*, Rev. Sci. Instrum. **69**, 3780 (1998).
[19] D. F. Price *et al.*, Phys. Rev. Lett. **75**, 252 (1995).
[20] Kent Estabrook and W. L. Kruer, Phys. Rev. Lett. **40**, 42 (1978).
[21] F. Brunel, Phys. Rev. Lett. **59**, 52 (1987).
[22] S. C. Wilks *et al.*, Phys. Rev. Lett. **69**, 1383 (1996).
[23] G. Malka *et al.*, Phys. Rev. Lett. **79**, 2053 (1997).
[24] J. P. Freidberg *et al.*, Phys. Rev. Lett. **28**, 795 (1972).
[25] Paul Gibbon and A. R. Bell, Phys. Rev. Lett. **68**, 1535 (1992).
[26] A. Djaoui and S. J. Rose, J. Phys. B **25**, 2745 (1992).